

Structural phase transition of graphene caused by GaN epitaxy

Y. Gohda and S. Tsuneyuki

Citation: *Appl. Phys. Lett.* **100**, 053111 (2012); doi: 10.1063/1.3680100

View online: <http://dx.doi.org/10.1063/1.3680100>

View Table of Contents: <http://apl.aip.org/resource/1/APPLAB/v100/i5>

Published by the [American Institute of Physics](#).

Related Articles

Geometric-shape-dependent structural transition behavior in (110) SrRuO₃ epitaxial thin films
J. Appl. Phys. **111**, 093532 (2012)

Nanocrystalline-to-amorphous transition in nanolaminates grown by low temperature atomic layer deposition and related mechanical properties
Appl. Phys. Lett. **100**, 191912 (2012)

Effect of gold composition on the orientations of oxide nuclei during the early stage oxidation of Cu-Au alloys
J. Appl. Phys. **111**, 083533 (2012)

Surface-induced phase behavior of polymer/nanoparticle blends with attractions
J. Chem. Phys. **136**, 164904 (2012)

In-situ neutron diffraction study of Pb(In_{1/2}Nb_{1/2})O₃-Pb(Mg_{1/3}Nb_{2/3})O₃-PbTiO₃ single crystals under uniaxial mechanical stress
J. Appl. Phys. **111**, 084110 (2012)

Additional information on *Appl. Phys. Lett.*

Journal Homepage: <http://apl.aip.org/>

Journal Information: http://apl.aip.org/about/about_the_journal

Top downloads: http://apl.aip.org/features/most_downloaded

Information for Authors: <http://apl.aip.org/authors>

ADVERTISEMENT



Goodfellow
metals • ceramics • polymers • composites
70,000 products
450 different materials
small quantities fast

www.goodfellowusa.com

Structural phase transition of graphene caused by GaN epitaxy

Y. Gohda^{1,a)} and S. Tsuneyuki^{1,2}

¹Department of Physics, The University of Tokyo, Tokyo 113-0033, Japan

²Institute for Solid State Physics, The University of Tokyo, Kashiwa 277-8581, Japan

(Received 16 August 2011; accepted 9 January 2012; published online 31 January 2012)

We report first-principles predictions, where the structure of graphene changes drastically with the epitaxial growth of GaN (which has been performed experimentally). We identify GaN- $\sqrt{3} \times \sqrt{3}$ /graphene- 2×2 superstructure as the most probable interface atomic structure, where three C-C bonds are replaced with C-N-C bonds preserving the Dirac cones. As the GaN epitaxy proceeds expanding graphene gradually, the tensile strain for graphene is released suddenly by partial breaking of the C-bond network, attributable to the two-dimensionality of graphene. In contrast, graphene retains its honeycomb structure at the AlN-graphene interface. Both of GaN- and AlN-graphene interfaces exhibit spin polarization. © 2012 American Institute of Physics. [doi:10.1063/1.3680100]

Graphene, a single layer of graphite, is one of the most promising materials for future nanoelectronics, as it is a peculiar conductor with Dirac cones. For device applications, graphene is expected to be in contact with an insulator or semiconductor rather than in freestanding configurations. Graphite-semiconductor interfaces can be an important stage in the fabrication of graphene-semiconductor systems, for example by photoexfoliation¹ combined with mechanical cleavage. On graphite, GaN has been grown epitaxially by using pulsed laser deposition,² where electron diffraction patterns have revealed that the hexagonal network of the GaN bilayer is rotated by 30° from the hexagonal network of graphite. Cleaving graphite layers after depositing nitrides should provide graphene as a two-dimensional substrate with unprecedented properties. Theoretical studies have suggested that the GaN-graphene interface has a well-defined 1×1 structure with the lattice constant of the three-dimensional GaN.³ However, the lattice mismatch between graphene and GaN is extraordinary large, ~30%, which encourages to explore other stable interface structures.

Atomically controlled interfaces may exhibit two-dimensional electronic and magnetic properties, opening up alternative options in nanomagnetism.⁴ First-principles calculations have recently predicted intrinsic itinerant ferromagnetism at lattice-matched AlN/MgB₂ (0001) interfaces.⁵ Since this d^0 ferromagnetism⁶ comes from unsaturated N p states, nitride-graphene interfaces might also exhibit spin polarization. However, because metal-induced gap states^{7,8} could lead to screening effects that hinder spin polarization,⁵ simple speculation is not reliable in this case, and detailed calculations are needed.

In this work, we propose stable structures for nitride-graphene interfaces, where the nitride (0001) structure is rotated by 30° relative to the graphene substrate, forming GaN- $\sqrt{3} \times \sqrt{3}$ /graphene- 2×2 and AlN- $5\sqrt{3} \times 5\sqrt{3}$ /graphene- 11×11 superstructures. We find that the C-C σ bonds of graphene in the GaN-graphene system partially break upon lattice expansion by GaN growth, where the interface strain is

reduced significantly by chemical bonding between C and N atoms, attributable to the two-dimensionality of graphene. We also show that the GaN-graphene system exhibits superparamagnetism when a gate bias is applied.

First-principles calculations were performed on the basis of density functional theory within the generalized gradient approximation.⁹ Numerical pseudo-atomic orbitals were used as the basis sets combined with pseudopotentials as implemented in the OpenMX code.¹⁰ The semicore Ga $3d$ as well as Al $2p$ states were explicitly calculated as valence electrons. We used a periodic slab model for the nitride-graphene systems. The sampling of k points was made using a $7 \times 7 \times 1$ grid for the primitive interface unit cell consisting of nitride (0001)- $\sqrt{3} \times \sqrt{3}$ and graphene- 2×2 including 32 atoms. We have confirmed that the use of a thicker slab does not affect our conclusions. In addition, the $2 \times 2 \times 1$ k -point sets were used for GaN- $4\sqrt{3} \times 4\sqrt{3}$ /graphene- 9×9 (546 atoms) and AlN- $5\sqrt{3} \times 5\sqrt{3}$ /graphene- 11×11 (842 atoms) superstructures, where lattice mismatches are very small: 0.1% and 0.4%, respectively. For other superstructures examined, the number of k points was scaled consistently. The nitride ultrathin films are N-polar with the (000 $\bar{1}$) surface at the opposite side of the interface as identified in the previous studies.^{2,3} The effective exchange couplings J_{ij} between sites i and j are calculated by perturbation theory with respect to spin fluctuation using the rigid-spin ansatz as follows:^{11,12}

$$J_{ij} = \frac{1}{2\pi} \int_{-\epsilon_F}^{\epsilon_F} d\epsilon \text{Tr}[\hat{G}_{ij}^\dagger \hat{V}_j \hat{G}_{ji}^\dagger \hat{V}_i],$$

where \hat{G}_{ij}^σ is the single-particle Green's function and \hat{V}_i is the on-site exchange interaction potential.¹²

Since it has been reported that the hexagons of GaN and graphene are rotated by 30° relative to one another, we examined so-called $\sqrt{3} \times \sqrt{3}$ structures, mainly nitride- $\sqrt{3} \times \sqrt{3}$ /graphene- 2×2 as well as GaN- $4\sqrt{3} \times 4\sqrt{3}$ /graphene- 9×9 and AlN- $5\sqrt{3} \times 5\sqrt{3}$ /graphene- 11×11 . The latter two structures are practically lattice-matched

^{a)}Electronic mail: gohda@phys.s.u-tokyo.ac.jp.

(mismatches less than 0.5%). In contrast, all of the N dangling bonds at the interfaces are expected to be saturated due to well-ordered structures for nitride- $\sqrt{3} \times \sqrt{3}$ /graphene- 2×2 interfaces, even though strain due to the lattice mismatch exists. Still, the lattice mismatch is greatly reduced to 12% for GaN and 9.5% for AlN compared with the 1×1 structure. The lattice mismatch can be effectively further reduced because of the C-C bond breaking and the two-dimensional nature of graphene as explained below. The interface N atoms are most stably located near the C-C bridge sites. The binding energies per interface N atom are 1.73 eV for GaN and 1.51 eV for AlN, much stronger than ~ 0.2 eV of the GaN-graphene 1×1 interface. As for the GaN- $4\sqrt{3} \times 4\sqrt{3}$ /graphene- 9×9 and AlN- $5\sqrt{3} \times 5\sqrt{3}$ /graphene- 11×11 interfaces, it is obtained as 1.27 eV and 1.82 eV, respectively. Other $\sqrt{3} \times \sqrt{3}$ superstructures available with our computational resources have lattice mismatches larger than 12% or negative ones (i.e., graphene with smaller lattice constant is compressed), except for $7 \times 7/5\sqrt{3} \times 5\sqrt{3}$ for GaN (AlN) with the mismatch of 4.8% (2.2%) having the binding energy of 1.55 eV (1.81 eV), respectively. Furthermore, we also examined the following superstructures (even though they contradict experiments), but all of them were identified as metastable: GaN- 4×4 /graphene- 5×5 , GaN- 7×7 /graphene- 9×9 , and AlN- 4×4 /graphene- 5×5 . Therefore, the most stable structures obtained in the present investigations are GaN- $\sqrt{3} \times \sqrt{3}$ /graphene- 2×2 and AlN- $5\sqrt{3} \times 5\sqrt{3}$ /graphene- 11×11 .

For nitride- $\sqrt{3} \times \sqrt{3}$ /graphene- 2×2 interfaces, we have found two atomic structures depending on the lattice constant as shown in Fig. 1. The initial structures for the optimization were interfaces consisting of bulk structures of nitrides and graphene that had been strained in accordance with the lattice constant. For smaller lattice constants, the hexagonal structure of graphene is preserved, whereas three of 12 C-C σ bonds are broken as the lattice constant becomes larger than 5.46 Å, resulting in the involvement of C-N-C bonds in the bond-network of C atoms.

Figure 2 shows the dependence of the total energy on the lattice constant. As the lattice constant increased gradually by

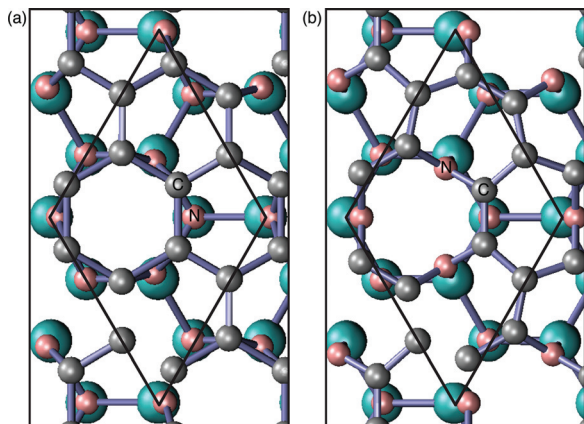


FIG. 1. (Color) Optimized atomic structures of nitride- $\sqrt{3} \times \sqrt{3}$ /graphene- 2×2 interfaces obtained for lattice constants (a) smaller than 5.46 Å and (b) larger than 5.46 Å. The largest balls represent group-III elements, either Al or Ga. The primitive unit cell is indicated by the solid rhombus.

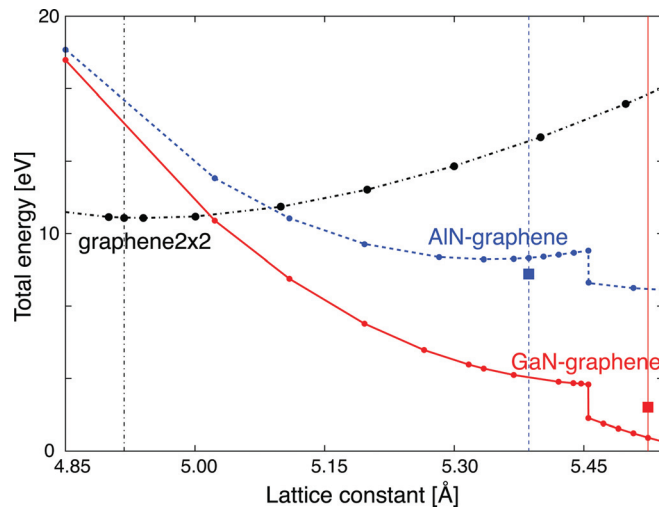


FIG. 2. (Color) Dependence of the total energy on the lateral lattice constant. Curves with balls for nitride-graphene are for nitride- $\sqrt{3} \times \sqrt{3}$ /graphene- 2×2 systems, whereas the two squares represent lattice-matched GaN- $4\sqrt{3} \times 4\sqrt{3}$ /graphene- 9×9 and AlN- $5\sqrt{3} \times 5\sqrt{3}$ /graphene- 11×11 . The origins of the energy for graphene, GaN-graphene, and AlN-graphene are arbitrary with each other. Lattice constants of graphene- 2×2 (4.92 Å), AlN- $\sqrt{3} \times \sqrt{3}$ bulk (5.39 Å), and GaN- $\sqrt{3} \times \sqrt{3}$ bulk (5.53 Å) are indicated by vertical lines.

the growth of nitrides, a structural phase transition from the structure in Fig. 1(a) to the one in Fig. 1(b) occurred when the lattice constant reached 5.46 Å, where the graphene sheet was stretched by 11%. For interfaces with lattice constants larger than 5.46 Å, the lattice mismatch is effectively much smaller than apparent ones, since the C-C bonds of graphene are partially broken upon the formation of the interface. Due to this reduction of the effective strain, the GaN- $\sqrt{3} \times \sqrt{3}$ /graphene- 2×2 interface is more stable than lattice-matched GaN- $4\sqrt{3} \times 4\sqrt{3}$ /graphene- 9×9 (Fig. 2, square). It should be noted that, as the thickness of nitride ultrathin films becomes larger, the lattice constant with the minimum total energy for the nitride-graphene system converges upon the lattice constant of bulk nitride. As has been already discussed,³ the interaction among graphite layers is considerably weak, so that the lattice constant of each graphite layer is independent with each other. Due to the two-dimensionality of single graphite layer (i.e., the graphene layer), the lattice constant of the interface structure is increased gradually by the growth of nitrides, and finally dominated by the three-dimensional nitride. Thus, lattice constants of bulk nitride are used in the calculations reported below.

The structural phase transition of the GaN-graphene system modifies the electronic structure. The lateral band structure is shown in Fig. 3(a). The existence of Dirac cones is clearly seen at the K point in the lateral Brillouin zone just above the Fermi level ϵ_F , even though the honeycomb network of C atoms is broken at the GaN-graphene interface. The existence of the Dirac cones, which is guaranteed by the chiral symmetry¹³ of the system, means that the π -bond network of graphene is preserved. There are spin-polarized bands at ~ -0.6 eV for the majority (up) spin and at ~ -0.1 eV for the minority (down) spin. Spin polarization of the GaN-graphene interface is mainly attributed to N $p_{||}$

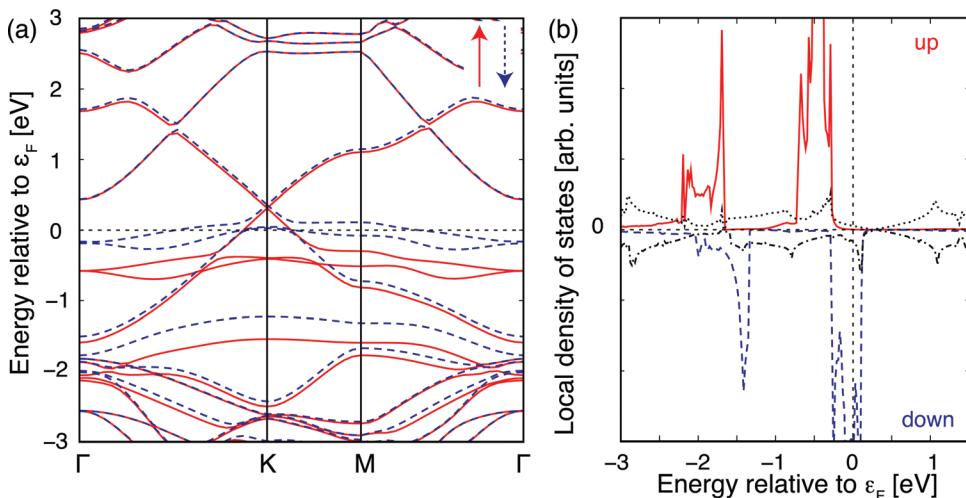


FIG. 3. (Color) (a) Electronic band structure for the GaN- $\sqrt{3} \times \sqrt{3}$ /graphene- 2×2 interface. (b) Local densities of states calculated by projecting onto interface-N $p_{||}$ states (solid and dashed curves, color) as well as p_z states of C atoms without direct bonding with N (dotted and dash-dotted curves, black).

states parallel to the interface, although significant hybridization with other states, especially the p_z states (perpendicular to the interface) of C atoms that do not bind with N atoms, is indeed obtained [Fig. 3(b)]. The orientation of the N $p_{||}$ states mentioned above is perpendicular to the sp^2 -like bond configuration of the N atoms.

The magnetization should be controllable by the gate bias voltage. Here, we injected extra charge into the system, which alters the occupancy of the interface states. Changes in the electronic states and the atomic structure due to the charging are calculated self-consistently. Figure 4(a) shows the dependence of the magnetic moment μ in the ground state on the injected charge q . The magnetization of GaN-graphene increases as the interface is positively charged. This feature coincides with the band structure shown in Fig. 3: the up-spin N $p_{||}$ states at ~ -0.6 eV are fully occupied, while the occupancy of the down-spin N $p_{||}$ states at ~ -0.1 eV is partial.

Figure 4(b) shows the dependence of J_{0j} on the distance between sites 0, one of the interface N atoms, and j at two different charge states. For $q = 1.5e$ (per primitive cell), fer-

romagnetic coupling among the three interface N atoms within the primitive cell shown in Fig. 1(b) is strong with $J_{0j} = 24$ meV, much stronger than that for the neutral charge state. Indeed the distance between these N atoms is $r_{0j} = 2.6$ Å which is significantly shorter than that in the bulk, 3.2 Å. This is in remarkable contrast with the case of cation vacancies in GaN,^{14,15} where breathing relaxation increases the distance between the N atoms with dangling bonds. However, the exchange coupling with other sites is negligibly small, which means that the GaN-graphene system with the charge state of $q = 1.5e$ should exhibit superparamagnetism.

As for AlN-graphene interfaces, structural phase transition of graphene does not occur as is shown in Fig. 2, because tensile strain for graphene is not large enough. Even though the honeycomb network is kept and apparently no dangling bonds are seen, spin polarization is also found for AlN-graphene. Qualitatively similar to GaN-graphene, spin-polarized states consist of interface-N $p_{||}$ states and p_z states of C without direct bonding with N, but the contribution from N $p_{||}$ states is quantitatively much weaker.

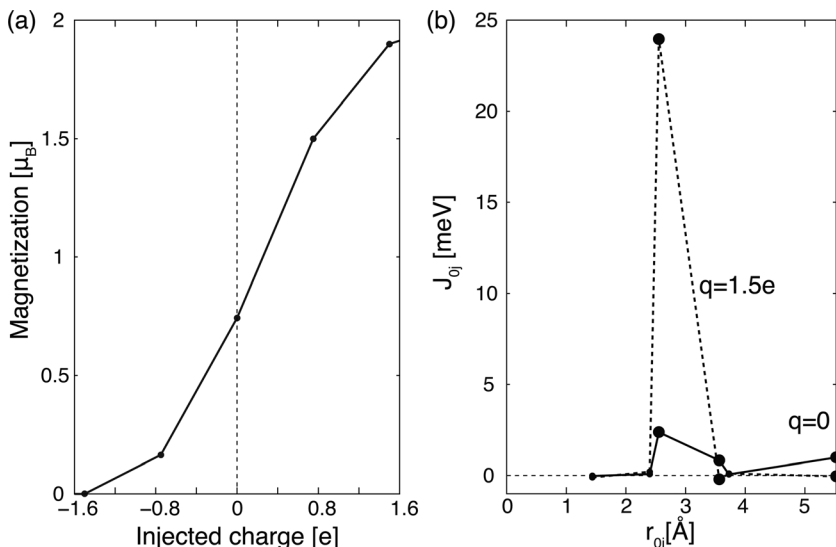


FIG. 4. (a) Dependence of the magnetic moment μ on the injected charge q calculated using the primitive interface unit cell of the GaN- $\sqrt{3} \times \sqrt{3}$ /graphene- 2×2 interface. (b) Effective exchange-coupling constants J_{0j} of GaN-graphene calculated with a rectangular unit cell containing two primitive cells, where site 0 is taken as one of the interface N atoms. Values for N-N (N-C) coupling are indicated by large (small) dots, respectively.

In conclusion, we predict structures of nitride-graphene interfaces. When the periodicity is $\sqrt{3} \times \sqrt{3}$ for GaN and 2×2 for graphene, the GaN-graphene interface is effectively nearly lattice-matched. The interface structure drastically changes, as the lattice is expanded by the growth of GaN. The GaN-graphene interface becomes superparamagnetic upon application of a gate bias. Such a structure is of potential importance also for applications to future nanoscale solar cells with a transparent graphene electrode.

This work has been supported by Grants-in-Aid for Scientific Research through Contract Nos. 21710102 and 22104006 as well as Next Generation Supercomputing Project, Nanoscience Program from MEXT, Japan. Calculations were partly performed using supercomputers at ISSP and ITC, The University of Tokyo.

¹Y. Miyamoto, H. Zhang, and D. Tománek, *Phys. Rev. Lett.* **104**, 208302 (2010).

²J. Ohta and H. Fujioka, "Growth of GaN on graphite by pulsed laser deposition" (unpublished).

³A. Ishii, T. Tatani, H. Asano, and K. Nakada, *Phys. Status Solidi C* **7**, 347 (2010); A. Ishii, T. Tatani, and K. Nakada, *ibid.* **8**, 1585 (2011).

⁴J. M. D. Coey, *Magnetism and Magnetic Materials* (Cambridge University Press, Cambridge, 2010).

⁵Y. Gohda and S. Tsuneyuki, *Phys. Rev. Lett.* **106**, 047201 (2011).

⁶J. M. D. Coey, *Solid State Sci.* **7**, 660 (2005).

⁷S. G. Louie and M. L. Cohen, *Phys. Rev. B* **13**, 2461 (1976).

⁸Y. Gohda, S. Watanabe, and A. Groß, *Phys. Rev. Lett.* **101**, 166801 (2008).

⁹J. P. Perdew, K. Burke, and M. Ernzerhof, *Phys. Rev. Lett.* **77**, 3865 (1996).

¹⁰T. Ozaki, *Phys. Rev. B* **67**, 155108 (2003).

¹¹A. I. Liechtenstein, M. I. Katsnelson, V. P. Antropov, and V. A. Gubanov, *J. Magn. Magn. Mater.* **67**, 65 (1987); V. P. Antropov, M. I. Katsnelson, and A. I. Liechtenstein, *Physica B* **237–238**, 336 (1997).

¹²M. J. Han, T. Ozaki, and J. Yu, *Phys. Rev. B* **70**, 184421 (2004); *ibid.* **75**, 060404(R) (2007).

¹³H. Watanabe, Y. Hatsugai, and H. Aoki, *Phys. Rev. B* **82**, 241403(R) (2010).

¹⁴Y. Gohda and A. Oshiyama, *Phys. Rev. B* **78**, 161201(R) (2008).

¹⁵Y. Gohda and A. Oshiyama, *J. Phys. Soc. Jpn.* **79**, 083705 (2010).